

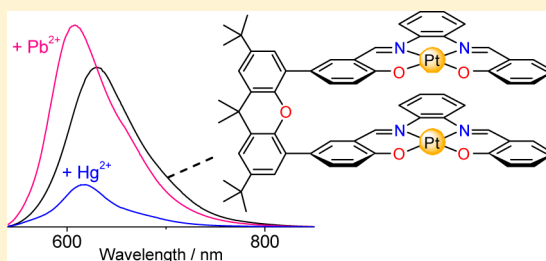
## Crowded Bis-(M-salphen) [M = Pt(II), Zn(II)] Coordination Architectures: Luminescent Properties and Ion-Selective Responses

Wah-Leung Tong, Shek-Man Yiu, and Michael C. W. Chan\*

Department of Biology and Chemistry, City University of Hong Kong, Tat Chee Avenue, Kowloon, Hong Kong, China

## S Supporting Information

**ABSTRACT:** For binuclear luminescent host systems, cooperativity between metal–organic moieties becomes feasible with regards to photophysical properties and sensing behavior. A new class of conformationally rigid binuclear platinum(II) and zinc(II) complexes bearing tetradentate aromatic Schiff base (salphen) ligands with limited rotational freedom has been prepared and characterized, and the molecular structure of a (Pt-salphen)<sub>2</sub> derivative has been determined by X-ray crystallography. Their UV–vis absorption and emission properties have been investigated and are tentatively ascribed to different excited states depending on the metal and the extent of intramolecular  $\pi$ -stacking interactions. Colorimetric and phosphorescent responses by the bis-Pt(II) complexes in the presence of selected metal ions have been observed. The nature of the host–guest interactions has been examined by quantitative binding studies, mass spectrometry and DFT calculations, and through comparisons with control complexes.

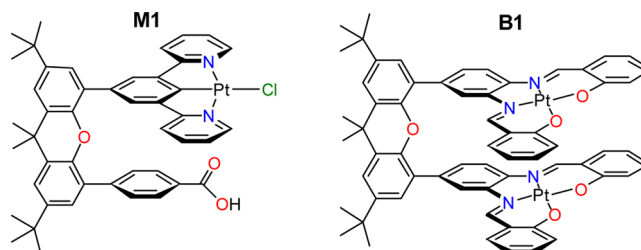


## ■ INTRODUCTION

Researchers have judiciously examined molecular phenomena such as restricted rotation, rigidization, and supramolecular attraction in crowded and shape-persistent aromatic frameworks in search of desirable recognition and signaling,<sup>1</sup> electronic,<sup>2</sup> and catalytic properties.<sup>3</sup> While reports on fluorescent systems have appeared,<sup>4</sup> the incorporation of luminescent metal–organic and phosphorescent components, which can confer attractive characteristics such as well-defined coordination geometries and visible-light signaling, have generally been overlooked. The emergence of metal–Schiff base complexes as important coordination and supramolecular motifs stems from their structural diversity coupled with functionality.<sup>5</sup> Considerable efforts have been devoted to the construction of Schiff base host architectures,<sup>6</sup> while their ion binding/transport,<sup>7</sup> chiral recognition,<sup>8</sup> and materials<sup>9</sup> applications, plus their aggregation into supramolecular assemblies and nanostructures, have been investigated.<sup>10,11</sup>

We are engaged in the development of shape-persistent phosphorescent host structures<sup>12</sup> and materials<sup>13</sup> containing environmentally responsive Pt(II) reporting units. For example, a new class of congested mononuclear Pt(II) ditopic frameworks was designed and synthesized, and investigations into their luminescent responses to amino acids revealed the ability to differentiate aminothiols, as well as preferential binding of the more sterically hindered cysteine over homocysteine to host **M1** (Chart 1).<sup>14</sup> For binuclear host complexes, cooperativity between the metal–organic moieties becomes feasible with regards to photophysical and sensing characteristics. We recently described a series of cofacial (Pt-salphen)<sub>2</sub> (H<sub>2</sub>salphen = *N,N'*-bis(salicylidene)-1,2-phenylenediamine) host assemblies anchored at each diimine phenyl ring to a rigid backbone component

Chart 1. Previously Developed Shape-Persistent Mono- and Binuclear Pt(II) Host Complexes

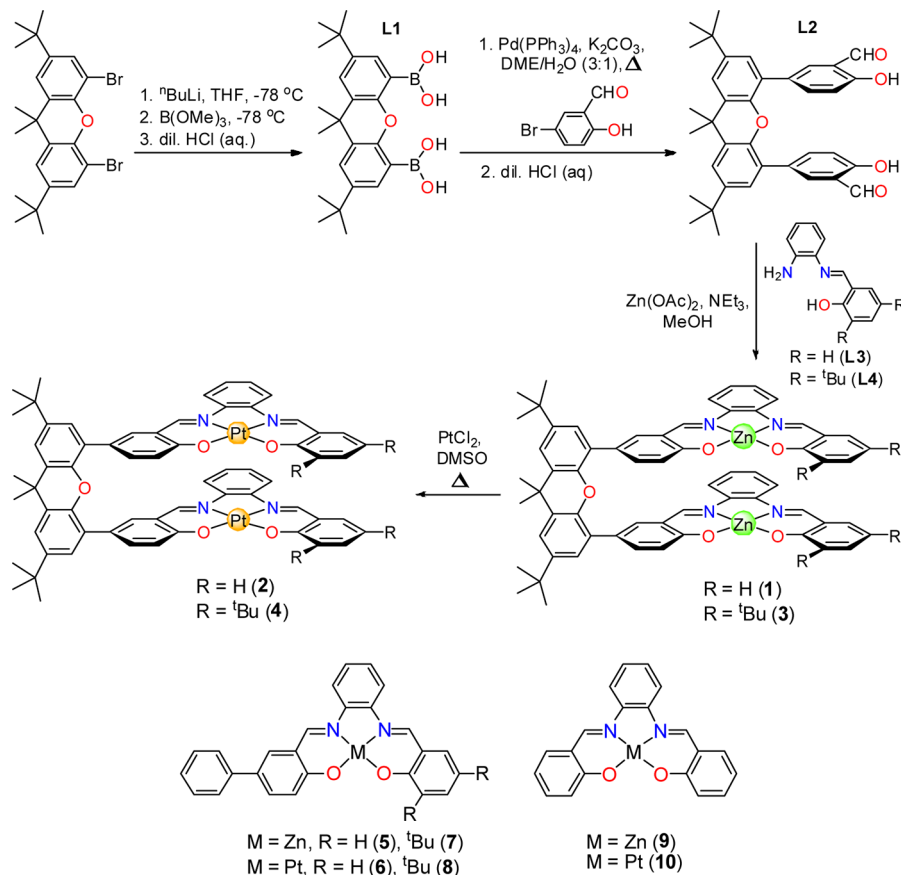


(xanthene (**B1** in Chart 1), biphenylene, or dibenzofuran), and their colorimetric and luminescent (in some case selective) responses to metal ions.<sup>15</sup> The employment of square planar Pt(II) luminophores can engender attractive properties such as tunable excited states that are highly sensitive to the micro-environment,<sup>16</sup> and Pt-salphen derivatives have been reported to exhibit high quantum efficiencies under ambient conditions.<sup>17</sup> Importantly, these frameworks were designed so that variations in molecular conformations are effectively limited to axial rotations of the Pt-salphen units. Nevertheless, such rotations can alter the intermetallic separations and possible intramolecular  $\pi$ -stacking interactions, as well as the distances and geometry between the pairs of O(salphen) donor atoms and hence the dimensions of the potential O<sub>4</sub>-binding pocket.

In this work, our aims are (a) to rearrange the host architecture by anchoring the Pt-salphen moieties at a phenoxy ring, to modify rotational flexibility and hence the extent of  $\pi$ -stacking

Received: March 20, 2013

**Scheme 1. Synthesis of Binuclear Complexes 1–4 and Structures of Control Complexes 5–10**



interactions and relative geometry of the cofacial luminophore units (and the resultant binding pocket), and (b) to probe the impact of these structural changes upon  $M^{n+}$ -binding characteristics. The luminescent and colorimetric responses of these di-Pt(II) frameworks, and their zinc(II) precursors, to metal ions have been investigated. In addition, their binding behavior with regards to selected metal ions has been examined by ESI-MS and DFT calculations, and comparatively studies with control complexes (bearing *t*-butyl substituents ortho to the O(salphen) atoms, and mononuclear analogues) have been performed, in order to rationalize the photophysical changes and offer insight toward a viable binding mechanism.

## ■ RESULTS AND DISCUSSION

**Synthesis and Structural Characterization.** The binuclear complexes **1–4** (Scheme 1) were prepared from the 4,5-dibromoxanthene precursor by substitution with bis-boronic acid (**L1**), followed by Pd-catalyzed coupling with 5-bromosalicylaldehyde at elevated temperature to give the ligand precursor **L2**. Next, the condensation between **L2** and the “semi-Schiff base” (**L3** or **L4**) was attempted, but isolation and purification of the desired bis-salphen ligand, which would allow direct metalation reactions, proved problematic. Instead, a Zn-templated, one-pot procedure<sup>18</sup> was adopted to afford the binuclear (Zn-salphen)<sub>2</sub> complexes **1** and **3**, which subsequently served as synthetic precursors to the Pt<sub>2</sub> complexes **2** and **4** through transmetalation reactions.<sup>19,20</sup> PtCl<sub>2</sub> was preferred to K<sub>2</sub>PtCl<sub>4</sub> as the metal source because the former is known for faster reactivity. The presence of *tert*-butyl substituents in **3** and **4** confers enhanced solubility in organic solvents compared with **1** and **2**. The mononuclear Zn (**5**)

and 7) and Pt (6 and 8) derivatives, which serve as control compounds for comparative studies, were similarly synthesized using the Zn-templated and transmetalation methods, respectively. The parent Zn- (9)<sup>21</sup> and Pt-salphen (10)<sup>17</sup> complexes were prepared according to literature reports. Complexes 1–8 were characterized by NMR spectroscopy, ESI–MS, and elemental analysis. Studies by ESI–MS revealed parent peak clusters with *m/z* values that correspond closely to the respective calculated isotopic patterns (Supporting Information).

Single crystals of **4**, **7**, and **8** were obtained by slow evaporation of  $\text{CH}_2\text{Cl}_2/\text{CH}_3\text{CN}$ ,  $\text{CH}_2\text{Cl}_2$ , and ethyl acetate solutions, respectively, and their molecular structures have been determined by X-ray crystallography (Supporting Information). Regarding the binuclear complex **4** (Figure 1), each platinum atom displays square planar geometry with minimal deviation of the salphen rings from the respective  $\text{Pt}(\text{N}_2\text{O}_2)$  planes. Mean Pt–N and Pt–O distances of 1.957 and 1.990 Å, respectively, are observed, which resemble those previously reported for Pt Schiff base complexes.<sup>17</sup> The two Pt-salphen moieties are linked to the xanthene bridge in a syn cofacial fashion, with dihedral angles (aryl-to-aryl) of 52.7° and 53.2° to the xanthene unit. The intramolecular interplanar separation (defined as mean separation between Pt and adjacent  $\text{N}_2\text{O}_2$  plane) of 3.67 Å, plus the non-coplanarity of the  $\text{N}_2\text{O}_2$  plane (angle = 12.6°), signify the absence of intramolecular  $\pi$ – $\pi$  interactions. This can be attributed to the steric impact of the *t*-butyl groups, although crystal packing effects should not be disregarded. Intramolecular Pt⋯Pt interactions<sup>22</sup> are also absent, as revealed by the Pt1⋯Pt2 distance of 4.855(2) Å. Such repulsive effects are avoided intermolecularly by a head-to-tail packing arrangement to afford

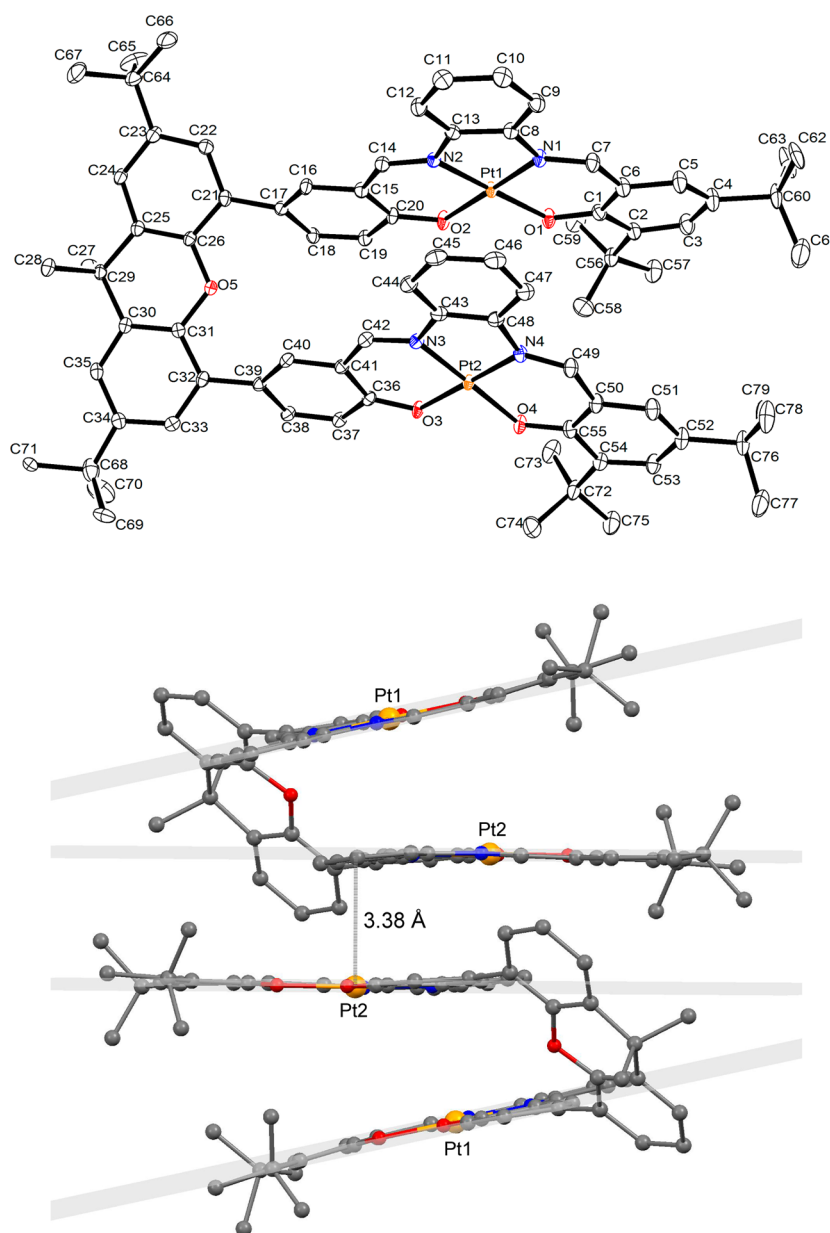


**Figure 1.** Molecular structure of **4**. Top: Perspective view (30% probability ellipsoids). Selected bond lengths (Å) and angles (deg): Pt1–O1 1.983(2), Pt1–O2 2.000(2), Pt1–N1 1.966(3), Pt1–N2 1.950(3), Pt2–O4 1.981(2), Pt2–O3 1.996(2), Pt2–N4 1.962(3), Pt2–N3 1.952(3), Pt1...Pt2 4.855(2); O1–Pt1–O2 85.52(10), N1–Pt1–O1 95.28(11), N2–Pt1–N1 83.36(12), N1–Pt1–O2 179.13(9). Bottom: Packing diagram (*t*Bu groups on backbone omitted for clarity) showing intermolecular  $\pi$ – $\pi$  separation.

intermolecular  $\pi$ -stacking interactions<sup>16a,23</sup> (interplanar separation = 3.38 Å between parallel  $N_2O_2$  planes; bottom of Figure 1). Like **4**, the molecular structure of the mononuclear congener **8** displays a head-to-tail crystal packing array, as well as interplanar separations of around 3.3 Å between parallel  $N_2O_2$  planes that are indicative of intermolecular  $\pi$ -stacking (Supporting Information). The square planar geometry at the Pt atom is unremarkable in **8**, and deviation of the salphen rings from the  $Pt(N_2O_2)$  plane is only slight.

Complex **7** was recrystallized from  $CH_2Cl_2$  to give a dimeric structure (Figure 2), in which an O(salphen) atom in one molecule acts as a bridge and coordinates to the Lewis acidic Zn center of the adjacent molecule ( $Zn1-O1^i$  2.064(1) Å) to give a  $Zn_2O_2$  parallelogram, with  $O1-Zn1-O1^i$  and  $Zn1-O1-Zn1^i$  angles of 82.94(4)° and 97.11(4)° respectively. The reliance of molecular structure upon the solvent used for recrystallization

has been reported for Zn-Schiff base complexes.<sup>11,24</sup> Within each monomeric unit, a distorted tetragonal pyramidal geometry<sup>25</sup> is evident for the Zn atom, and the Zn–O bond for the nonbridging O atom ( $Zn1-O2$  1.944(1) Å) is noticeably shorter than that for the bridging O atom ( $Zn1-O1$  2.042(1) Å). An antiparallel arrangement is adopted, so as to minimize repulsion between the *t*-butyl substituents. The dimeric molecular structure of **7** emphasizes the coordinating ability of the O(salphen) moieties in such complexes. These structural observations may be useful for rationalizing the experimental findings (including luminescent behavior) in this work.

**Absorption and Emission Spectroscopy.** The photophysical properties of the Pt (Figure 3 and Table 1) and Zn (Figure 4 and Supporting Information) complexes have been studied by UV–vis absorption and emission spectroscopy (photophysical data for **9**<sup>21</sup> and **10**<sup>17c</sup> have been reported

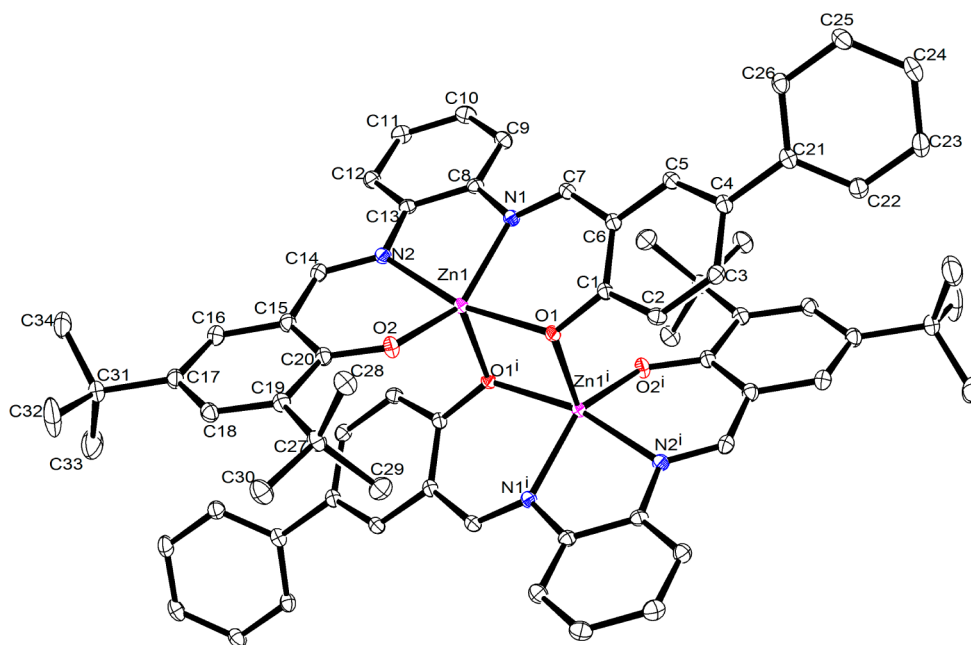


**Figure 2.** Perspective view of **7** (30% probability ellipsoids). Selected bond lengths (Å) and angles (deg): Zn1–Zn1<sup>i</sup> 3.0776(4), Zn1–O1<sup>i</sup> 2.064(1), Zn1–O1 2.042(1), Zn1–O2 1.944(1), Zn1–N1 2.083(1), Zn1–N2 2.070(1); Zn1–O1–Zn1<sup>i</sup> 97.11(4), O1–Zn1–O1<sup>i</sup> 82.89(4), O1–Zn1–N1 87.29(5), O1–Zn1–N2 165.75(5), O2–Zn1–N1 147.27(5), N2–Zn1–N1 78.73(5).

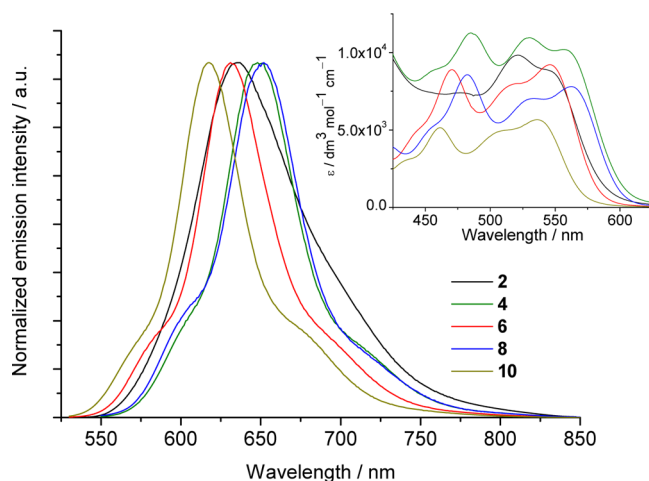


**Figure 3.** Normalized emission spectra (inset: low-energy UV-vis absorption bands) of Pt-salphen complexes in  $\text{CHCl}_3$  ( $10^{-5}$  M) at 298 K.

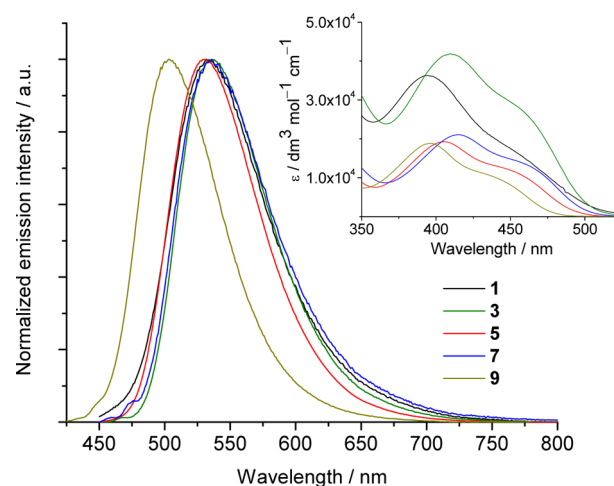


**Figure 4.** Normalized emission spectra (inset: low-energy UV-vis absorption bands) of Zn-salphen complexes in  $\text{CH}_3\text{CN}$  ( $10^{-5}$  M) at 298 K.

**Table 1.** Photophysical Data for (Pt-salphen)<sub>2</sub> Complexes **2** and **4** (and Mononuclear Controls **6** and **8**, Respectively)

compd	$\lambda_{\text{max}}/\text{nm}$ ( $\epsilon/\text{dm}^3 \text{ mol}^{-1} \text{ cm}^{-1}$ ) <sup>a</sup>	$\lambda_{\text{ex}}/\text{nm}$	fluid: $\lambda_{\text{max}}/\text{nm}$ ( $\tau/\mu\text{s}$ ); $\Phi$		solid: $\lambda_{\text{max}}/\text{nm}$ ( $\tau/\mu\text{s}$ )	
			298 K	77 K <sup>c</sup>	298 K	77 K
<b>2</b>	319 (55 490), 359 (47 150), 477 (7400), 521 (9830), 546 (8830)	521	635 <sup>a</sup> (2.1); 0.044 [630 <sup>b</sup> ]	590, 630 (max, 12), 683	650 (0.056)	665 (max, 1.5), 724
<b>4</b>	321 (59 100), 370 (49 000), 485 (11 280), 530 (10 960), 557 (10 190)	530	610, <sup>a</sup> 649 (max, 3.6), 701; 0.086 [603, <sup>b</sup> 643 (max), 699]	626 (max, 9.4), 687	648 (max, 0.16), 703	658 (max, 4.7), 723
<b>6</b>	291 (46 070), 366 (39 910), 385 (47 070), 470 (8890), 515 (7880), 546 (9210)	515	590, <sup>a</sup> 631 (max, 4.5), 683; 0.17 [578, <sup>b</sup> 625 (max), 675]	602 (max, 11), 660	659 (0.096)	676 (max, 2.4), 730
<b>8</b>	292 (39 310), 371 (34 330), 389 (39 070), 483 (8560), 535 (7030), 562 (7800)	532	612, <sup>a</sup> 652 (max, 3.3), 703; 0.11	613 (max, 9.0), 674	656 (max, 0.66), 705	653 (max, 4.1), 713

<sup>a</sup>In  $\text{CHCl}_3$ . <sup>b</sup>In  $\text{CHCl}_3/\text{CH}_3\text{CN}$  (1/1). <sup>c</sup>In  $n\text{BuCN}$ .



previously). The UV–vis absorption spectra of the Pt complexes contain intense bands at  $\lambda_{\text{max}} < 390 \text{ nm}$  ( $\epsilon > 2.5 \times 10^4 \text{ dm}^3 \text{ mol}^{-1} \text{ cm}^{-1}$ ) that are attributable to intraligand  $^1(\pi-\pi^*)$  transitions of the salphen ligands. The less intense absorption bands in the visible region (inset of Figure 3) are assigned to  $\text{O}(\text{p})/\text{Pt}(\text{d}) \rightarrow \pi^*(\text{diimine})$  transitions.<sup>17,26</sup> When compared with the parent salphen complex (**10**), the Pt derivatives in this work display red-shifted absorptions at  $\lambda_{\text{max}} 470\text{--}557 \text{ nm}$  ( $\epsilon = (7\text{--}11) \times 10^3 \text{ dm}^3 \text{ mol}^{-1} \text{ cm}^{-1}$ ), which can be ascribed to the electronic effects of the phenoxy substituents (aryl, *t*Bu).

The Pt complexes in this study display red emission ( $\lambda_{\text{max}} 631\text{--}652 \text{ nm}$ ) in  $\text{CHCl}_3$  at 298 K, which are assigned to mixed triplet  $\text{O}(\text{p})/\text{Pt}(\text{d}) \rightarrow \pi^*(\text{diimine})$  excited states (Figure 3). In general, the fluid emission undergoes a blue-shift in more polar medium as a consequence of the polar nature of the electron-rich oxygen donors in the ground state.<sup>17,26</sup> For example, the emission maximum for **2** at 637 nm in toluene is blue-shifted to 631 and 625 nm in  $\text{CH}_2\text{Cl}_2$  and DMSO, respectively (Supporting Information). Like the lowest-energy absorptions, the emissions of **2**, **4**, **6**, and **8** are red-shifted from that of the parent Pt-salphen (**10**;  $\lambda_{\text{max}} 617 \text{ nm}$ ). Hence, the phenyl/xanthene substituents on the phenoxy group in **2** and **6** ( $\lambda_{\text{max}} 634$  and  $631 \text{ nm}$  respectively) apparently destabilize the HOMO, while the additional red-shift for **4** and **8** ( $\lambda_{\text{max}} 649$  and  $652 \text{ nm}$ , respectively) can similarly be attributed to further HOMO destabilization due to the electron-donating effect of the *t*-butyl groups.

Although the emission maxima for **2** and **6** are similar, **2** displays a broader, less structured emission (full width at half-maximum =  $1940 \text{ cm}^{-1}$  ( $\nu_{604} - \nu_{684}$ ), compared with  $1320 \text{ cm}^{-1}$  ( $\nu_{608} - \nu_{661}$ ) for **6**), which is concentration-independent and tentatively ascribed to weak  $\pi$ -stacking interactions within the cofacial  $(\text{Pt-salphen})_2$  moiety. Such intramolecular interactions are known to cause self-quenching,<sup>1f,12a,22a</sup> and this is reflected by the lower luminescence quantum yield for **2** ( $\Phi = 0.044$  in  $\text{CHCl}_3$ , compared with 0.17 for **6**). On the contrary, the *t*Bu-substituted derivatives **4** and **8** show very similar emission profiles (in terms of energy and band shape) and only a minor difference in quantum yield, indicating that intramolecular  $\pi$ -interactions are absent presumably due to the repulsive effects of the *t*Bu groups. This conclusion is consistent with the observed large intramolecular separation and non-coplanarity of the Pt-salphen units in the crystal structure of **4**.

The 77 K glassy emissions of Pt complexes in *n*BuCN are blue-shifted (due to the Franck–Condon effect) and more structured compared with their respective solution emissions at 298 K, and excimeric emissions are not observed at a concentration of  $10^{-5} \text{ M}$ . The glassy emissions of **2** and **4** are red-shifted and broader compared with their respective mononuclear analogues **6** and **8** (Supporting Information), which may be tentatively attributed to a contraction of the rigid xanthene backbone possibly bringing the two tethered Pt-salphen moieties into closer proximity. The solid-state emissions are generally red-shifted and become less structured than their fluid emissions, presumably because of enhanced intra- (for **2** and **4**) and/or intermolecular  $\pi$ -stacking interactions.

The UV–vis absorption spectra of the Zn complexes in  $\text{CH}_3\text{CN}$  show intense bands at  $\lambda < 350 \text{ nm}$  ( $\epsilon > 4 \times 10^4 \text{ dm}^3 \text{ mol}^{-1} \text{ cm}^{-1}$ ) that are attributed to intraligand  $^1(\pi-\pi^*)$  transitions, while the low-energy absorptions at  $\lambda_{\text{max}} 375\text{--}500 \text{ nm}$  ( $\epsilon = (1\text{--}4) \times 10^4 \text{ dm}^3 \text{ mol}^{-1} \text{ cm}^{-1}$ ; inset of Figure 4) are tentatively assigned to  $\text{O}(\text{p}) \rightarrow \pi^*(\text{imine})$  intraligand charge transfer (ILCT) transitions, in accordance with previous studies of Zn-Schiff base complexes.<sup>27</sup> The Zn complexes in this work

display structureless emission in  $\text{CH}_3\text{CN}$  at 298 K (Figure 4), which are assigned to  $^1\text{IL}$  excited states with fluorescence lifetimes in the subnanosecond regime. Complexes **1**, **3**, **5**, and **7** emit at  $\lambda_{\text{max}} 530\text{--}538 \text{ nm}$ , which is red-shifted from the parent Zn-salphen **9** due to greater  $\pi$ -conjugation and substitution of the respective salphen ligands. The concentration dependence of the emission of **7** was investigated in  $\text{CHCl}_3$  (Supporting Information); the peak maximum appears at 545 nm at concentrations up to  $10^{-4} \text{ M}$ , but undergoes a slight red-shift to 550 nm at  $1 \times 10^{-3} \text{ M}$ . This behavior brings to mind the dimeric crystal structure of **7** and may be indicative of luminophore aggregation at relatively low concentrations in  $\text{CHCl}_3$  (indeed, a peak cluster corresponding to the calculated isotopic pattern for  $[(\text{7})_2 + \text{H}]^+$  was detected by ESI–MS; Supporting Information). The solid-state emissions of the Zn complexes are structureless at 298 and 77 K.

**Photophysical Responses to Metal Ions: Investigation of Binding Process and Comparative Studies.** The binding behavior of the binuclear complexes in the presence of metal ions (in the form of perchlorate salts) has been investigated by spectrophotometric titrations. For the  $(\text{Zn-salphen})_2$  complex **1**, varying emission responses without selectivity were obtained (Supporting Information: enhancement for  $\text{Mg}^{2+}$ ,  $\text{Ca}^{2+}$ ,  $\text{Cd}^{2+}$  (partial for  $\text{La}^{3+}$ ); minor quenching for  $\text{Cu}^{2+}$ ,  $\text{Hg}^{2+}$ ,  $\text{Pb}^{2+}$ ; minimal or no response for monovalent metals and  $\text{Zn}^{2+}$ ). Bearing in mind the established tendency of Zn-salphen complexes to undergo transmetalation processes,<sup>6e,19,20</sup> as observed in this work, and the reported facile formation of  $\text{Mg}(\text{II})$ ,  $\text{Ca}(\text{II})$ , and  $\text{Cd}(\text{II})$  Schiff base derivatives under ambient conditions,<sup>28</sup> the likelihood that **1** engages in alternative reactions<sup>29</sup> (other than binding) with multivalent cations therefore renders such Zn complexes unsuitable for further photophysical studies.

Interesting photophysical responses were observed for the  $\text{Pt}_2$  host **2** in the presence of various metal ions (1.0 equiv) in  $\text{CH}_3\text{CN}/\text{CHCl}_3$  (1/1). Upon addition of  $\text{Pb}^{2+}$ , minor emission enhancement was apparent and accompanied by a significant blue-shift ( $\lambda_{\text{max}} 630$  to  $605 \text{ nm}$ ). For  $\text{Hg}^{2+}$  and  $\text{Cu}^{2+}$ , the emission was quenched with minor blue-shifts in peak maximum, while minimal or no responses were detected for  $\text{Mg}^{2+}$ ,  $\text{Ca}^{2+}$ ,  $\text{Zn}^{2+}$ ,  $\text{Cd}^{2+}$ ,  $\text{La}^{3+}$ , and all monovalent metals ions (Figure 5). Competition experiments to study the ratiometric response of **2** to  $\text{Pb}^{2+}$  ions were conducted, revealing a degree of selectivity

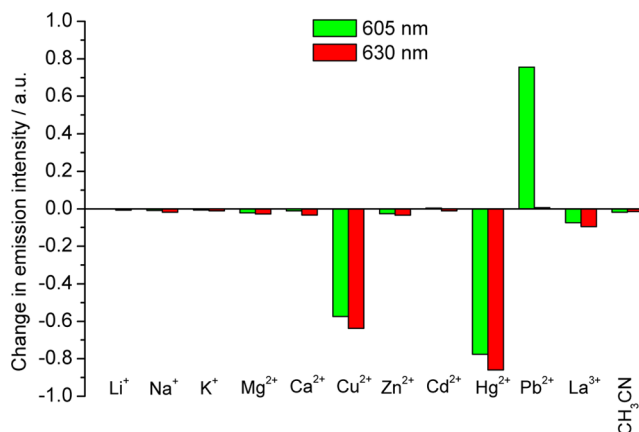


**Figure 5.** Change in emission intensity at 605 and 630 nm for **2** ( $2.0 \times 10^{-5} \text{ M}$ ;  $\lambda_{\text{ex}} 501 \text{ nm}$ ) upon addition of  $\text{M}^{n+}$  ions (1.0 equiv) in  $\text{CH}_3\text{CN}/\text{CHCl}_3$  (1/1).

toward  $\text{Pb}^{2+}$  with partial interference from  $\text{Cu}^{2+}$  and  $\text{Hg}^{2+}$  (Supporting Information).

Quantitative titrations have been performed to probe the spectroscopic response of **2** toward  $\text{Pb}^{2+}$  (top of Figure 6). The

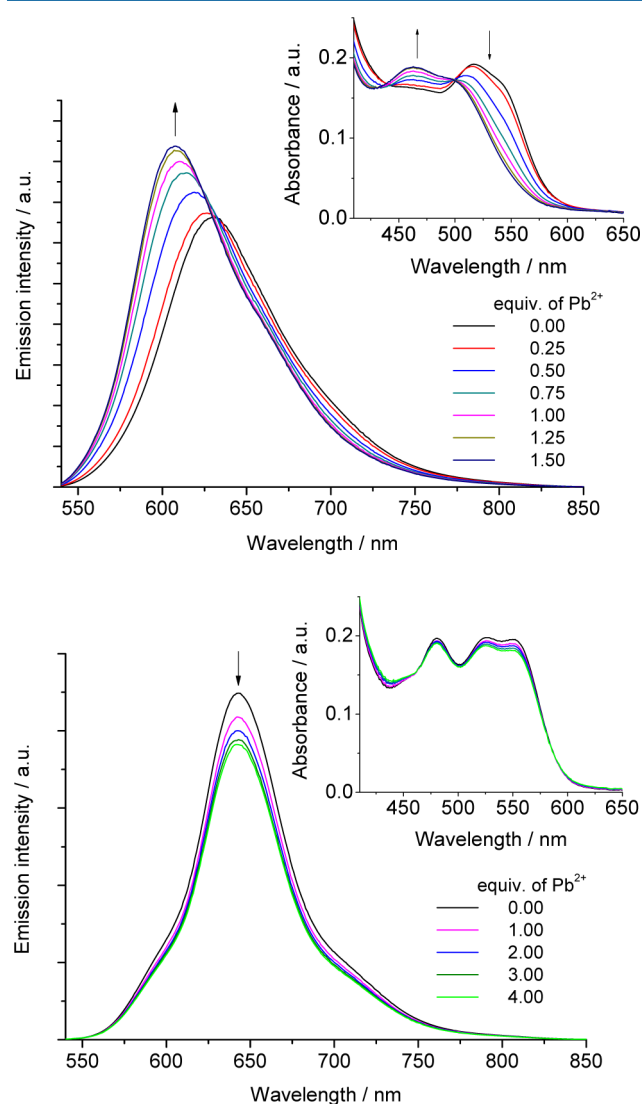


**Figure 6.** Quantitative emission (inset: expanded UV-vis) titrations of **2** (top) and <sup>t</sup>Bu-substituted analogue **4** (bottom; both  $2.0 \times 10^{-5}$  M) upon addition of  $\text{Pb}^{2+}$  in aerated  $\text{CH}_3\text{CN}/\text{CHCl}_3$  (1/1).

UV-vis spectral changes became saturated after addition of ca. 1 equiv of  $\text{Pb}^{2+}$ ; the absorption band at  $\lambda_{\text{max}}$  516 nm was blue-shifted to  $\lambda_{\text{max}}$  463 nm and a well-defined isosbestic point at 501 nm was observed, which was used as the excitation wavelength ( $\lambda_{\text{ex}}$ ) for emission studies. In the emission titration, incremental changes were detected for up to 1.0 equiv of  $\text{Pb}^{2+}$ , and this was followed by minor changes until saturation occurred for 1.5 equiv; hence, the structureless red emission at  $\lambda_{\text{max}}$  630 nm was blue-shifted to  $\lambda_{\text{max}}$  605 nm with partial enhancement (aerated quantum yield increased from  $4.9 \times 10^{-3}$  to  $6.8 \times 10^{-3}$ ), and the aerated emission lifetime became longer ( $\tau_{630} = 0.13 \mu\text{s}$ ;  $\tau_{605} = 0.30 \mu\text{s}$ ). Intriguingly, the resultant emission maximum of 605 nm is higher in energy than that (625 nm) for the mononuclear congener **6** (see discussion below).

Studies have been undertaken to gain insight into the binding mechanism for **2**. A Job's plot indicating 1:1 stoichiometry for

$\text{Pb}^{2+}$ -binding by **2** was obtained (Supporting Information). Moreover, the binding constant<sup>30</sup> was calculated from the emission intensity at 605 nm as a function of  $[\text{Pb}^{2+}]$ , and the log  $K$  was determined to be  $6.30 \pm 0.35$  in  $\text{CH}_3\text{CN}/\text{CHCl}_3$  (1/1); a comparison can be made to the closely related xanthene-linked (Pt-salphen)<sub>2</sub> complex **B1** (Chart 1) in  $\text{CH}_3\text{CN}/\text{CH}_2\text{Cl}_2$  (1/1; log  $K = 6.63 \pm 0.06$ ).<sup>15</sup> Quantitative spectroscopic titrations of **2** with  $\text{Pb}^{2+}$  in coordinating THF were performed to evaluate the relevance of the proposed binding by O(salphen) moieties (Supporting Information). Indeed, more subtle UV-vis and emission changes were detected upon addition of 5.0 equiv of  $\text{Pb}^{2+}$ , and a noticeably smaller binding constant (log  $K = 3.12 \pm 0.27$ ) was determined in THF than  $\text{CH}_3\text{CN}/\text{CH}_2\text{Cl}_2$ . These results signify that the THF solvent can interfere with the  $\text{Pb}^{2+}$ -binding process, although there are many contributing factors (such as solvation effects). The binding process for **2** was further investigated using ESI mass spectrometry. A major signal in the ESI mass spectrum of **2** with 1.0 equiv of  $\text{Pb}(\text{ClO}_4)_2$  in  $\text{CH}_3\text{CN}/\text{CHCl}_3$ , using zero declustering potential, was a cluster at  $m/z$  772.1 with peak separations of 0.5 amu, which is in excellent agreement with the calculated isotopic pattern for the  $[\text{2} + \text{Pb}]^{2+}$  (1:1) species.<sup>31</sup> Furthermore, a cluster at  $m/z$  1643.4 corresponding closely to  $[\text{2} + \text{Pb} + \text{ClO}_4]^+$  with 1 amu separations was also prominent (Figure 7), implying that when

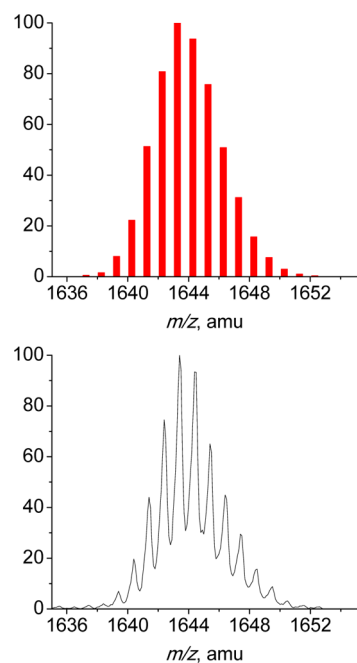


**Figure 7.** ESI-MS of  $[\text{2} + \text{Pb} + \text{ClO}_4]^+$  in  $\text{CH}_3\text{CN}/\text{CHCl}_3$  (1/1) using zero declustering potential (top: calculated isotopic distributions).

bound by **2**, the  $\text{Pb}^{2+}$  ion may also be coordinated by perchlorate. At this juncture, consideration for the related crystal structures of  $[\{\text{Ni}(\text{salen})\}_2 \cdot \text{Ba}(\text{ClO}_4)_2(\text{thf})]$  (featuring two chelating perchlorate groups at  $\text{Ba}^{2+}$  plus  $\text{O}_4$ -coordination by two mononuclear Ni-salen moieties)<sup>32</sup> and  $(\text{NBu}_4)[\{\text{bzq}\}\text{Pt}(\text{C}\equiv\text{CC}_6\text{H}_4\text{-4-CF}_3)_2\}_2 \cdot \text{Pb}(\text{ClO}_4)]$  (bzq = 7,8-benzoquinoline; the  $\text{Pb}^{2+}$  ion is coordinated by a bidentate perchlorate group, plus four acetylide moieties of two  $[(\text{bzq})\text{Pt}(\text{C}\equiv\text{CAr})_2]$  units in a  $[\eta^1(\text{C}\equiv\text{CAr})]_4$  binding mode),<sup>33</sup> plus the structurally characterized multidentate O-coordination of  $\text{M}(\text{OAc})_2$  ( $\text{M} = \text{Zn}, \text{Ni}$ ) by the O(salphen) and O-alkyl moieties of alkoxy-substituted M-salphen complexes,<sup>20</sup> is warranted. In contrast, signals

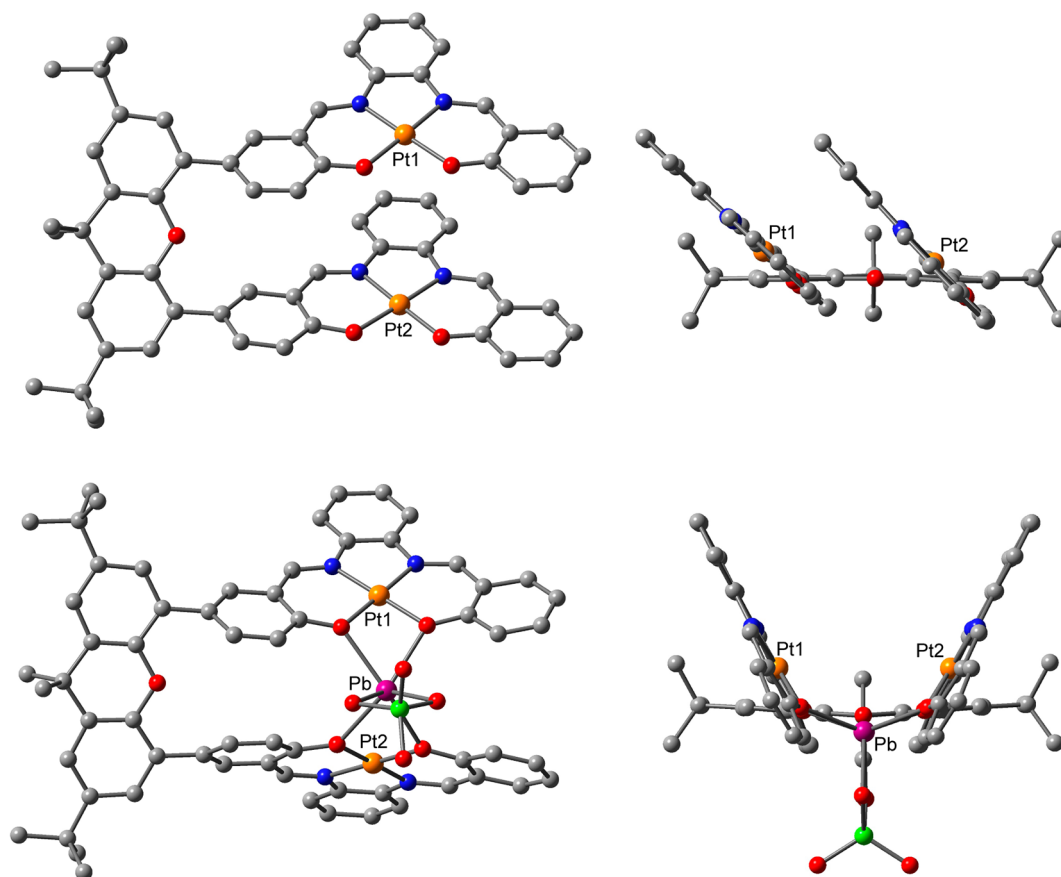


**Figure 8.** Perspective views of energy-minimized (Gaussian) calculated structure of **2** (top) and  $[2 + \text{Pb} + \text{ClO}_4]^+$  (bottom). Color legend: gray = C, blue = N, red = O, orange = Pt, green = Cl, and purple = Pb.

corresponding to analogous host–guest species were not observed for **2** with  $\text{Hg}(\text{ClO}_4)_2$  (1.0 equiv) under identical conditions.

Repeated attempts to grow crystals of **2** (including in the presence of various ratios of  $\text{Pb}(\text{ClO}_4)_2$ ) for structural elucidation have been unsuccessful. The structures of **2** and the  $[2 + \text{Pb} + \text{ClO}_4]^+$  species observed by ESI–MS have been optimized by density functional theory (DFT) calculations. The energy-minimized calculated structures were each confirmed to be a minimum from vibrational frequency calculations (Figure 8; see the Supporting Information for selected calculated bond lengths). The two Pt-salphen planes in **2** are arranged in a cofacial manner with dihedral angles (aryl-to-aryl) to the xanthene backbone of ca.  $45^\circ$ . The interplanar separation [mean  $\text{Pt}\cdots(\text{N}_2\text{O}_2 \text{ plane})$  distance] of  $3.59 \text{ \AA}$  and the angle of  $2.1^\circ$  between the  $\text{N}_2\text{O}_2$  planes indicate that weak  $\pi$ – $\pi$  interactions are plausible, which is consistent with the emissive properties, while the contrast with the structural parameters of **4** (without intramolecular  $\pi$ -interactions; corresponding separation and angle of  $3.67 \text{ \AA}$  and  $12.6^\circ$ , respectively) is clear. In the calculated structure of  $[2 + \text{Pb} + \text{ClO}_4]^+$ , the  $\text{Pb}^{2+}$  ion is located in the center of the  $\text{O}_4$ -binding pocket and is bound by a bidentate perchlorate group. Starting from the conformation of **2**, the Pt-salphen planes evidently undergo axial rotation with respect to the xanthene unit, and the angle between the  $\text{N}_2\text{O}_2$  planes increases to  $61.7^\circ$ , thus ensuring that any weak  $\pi$ -interaction is broken. The  $\text{Pb}^{2+}$ -bound Cl–O bonds (mean  $1.822 \text{ \AA}$ ) are longer than the nonchelating Cl–O bonds (mean  $1.730 \text{ \AA}$ ), while the mean Pt–O ( $2.042 \text{ \AA}$ ) and C–O ( $1.373 \text{ \AA}$ ) bond lengths are elongated

slightly (by  $0.010$  and  $0.034 \text{ \AA}$ , respectively). The Pb–O distances ( $2.469$ – $2.510 \text{ \AA}$ ) are comparable to literature reports of Pb–O bonds,<sup>34,35</sup> and the mean  $\text{Pb}\cdots\text{Pt}$  distance is  $3.397 \text{ \AA}$ . These results suggest that guest-induced conformational changes (i.e., axial rotation) for the Pt-salphen moieties in **2** can engender a viable  $\text{O}_4$ -binding site for a perchlorate-bound  $\text{Pb}^{2+}$  ion.

Comparisons with control complexes and further photo-physical studies have been undertaken to rationalize the spectral changes and binding mechanism for **2**. Upon addition of  $\text{Pb}^{2+}$ , the emission  $\lambda_{\text{max}}$  of **2** in  $\text{CHCl}_3/\text{CH}_3\text{CN}$  (1/1) blue-shifts to  $605 \text{ nm}$ , which is substantially higher in energy than that for the mononuclear congener **6** ( $625 \text{ nm}$ ). In addition to the consequence of breaking the weak intramolecular  $\pi$ -interactions (to afford monomer-like emission), we ascribe the “extended” blue-shift to the destabilization of the  $\text{O}(\text{p}) \rightarrow \pi^*(\text{diimine})$  transition arising from stabilization of salphen  $\text{O}(\text{p})$  orbitals upon  $\text{Pb}^{2+}$ -coordination, in a manner akin to that predicted by DFT calculations. Notably, this is entirely consistent with the observed blue-shift for the lowest-energy absorption band of **2** with increasing  $[\text{Pb}^{2+}]$  (top of Figure 6).

A comparison between **2** and its  $^t\text{Bu}$ -substituted analogue **4** is informative. Significantly, the addition of  $\text{Pb}^{2+}$  to **4** caused minor quenching of the relatively structured emission at  $\lambda_{\text{max}}$   $643 \text{ nm}$  in  $\text{CH}_3\text{CN}/\text{CHCl}_3$  (1/1) without any shift in peak maximum (bottom of Figure 6). The absence of intramolecular  $\pi$ -interactions in **4** (as evident from the crystal structure and emissive properties) is attributed to the influence of the  $^t\text{Bu}$  groups, and it is highly plausible that these bulky substituents adjacent to the  $\text{O}(\text{salphen})$  moieties could sterically hinder the



formation of the O<sub>4</sub>-cavity and possibly block the binding of guests (notwithstanding their electronic effects). The lack of a blue-shift for the UV–vis and emission bands of **4** with Pb<sup>2+</sup> is consistent with this and implies that coordination by the O(salphen) groups does not occur. Regarding the emission quenching, it is revealing to note that the responses of **4** and the mononuclear controls **6** and **10** are very similar (Supporting Information). Taken together, these observations signify that quenching via metallophilic or spin–orbit interactions<sup>36</sup> is the conventional luminescent response of mononuclear Pt-salphen to Pb<sup>2+</sup>, and tentatively suggest that the binding of Pb<sup>2+</sup> by **2** takes place inside the (Pt-salphen)<sub>2</sub> cavity to produce emission enhancement, while such binding behavior is prevented by the <sup>t</sup>Bu groups in **4**.

The following points should be emphasized when attempting to rationalize the observed photophysical changes: (a) a blue-shifted emission may be caused by (i) destabilization of the O(p)→ $\pi^*$ (diimine) transition upon Pb<sup>2+</sup>-binding, and/or (ii) disruption of weak  $\pi$ – $\pi$  interactions within the (Pt-salphen)<sub>2</sub> unit; (b) although Pb<sup>2+</sup> ions can invariably quench the emission of Pt-salphen luminophores, the observation of enhanced emission intensity upon Pb<sup>2+</sup>-binding may result from (i) reduction in intramolecular self-quenching due to weaker or cleaved  $\pi$ – $\pi$  interactions, and/or (ii) rigidization of the host framework. We therefore propose that, as shown by DFT calculations, the binding of Pb<sup>2+</sup> within the O<sub>4</sub>-cavity of **2** necessitates axial rotation of the cofacial Pt-salphen moieties and disruption of the weak intramolecular  $\pi$ – $\pi$  interactions that give rise to the emission at  $\lambda_{\text{max}}$  630 nm in CHCl<sub>3</sub>/CH<sub>3</sub>CN; consequently, the reduction in self-quenching and increased host rigidity would counterbalance the expected Pb<sup>2+</sup>-mediated quenching to yield enhanced (or undiminished) emission at  $\lambda_{\text{max}}$  605 nm.

The observed selectivity of **2** for Pb<sup>2+</sup> is tentatively ascribed to the nature of the O<sub>4</sub>-binding pocket, which apparently exhibits good size-complementarity for the Pb<sup>2+</sup> ion (radius = 1.19 Å),<sup>37</sup> as indicated by DFT. Although size-match should be an important factor, selectivity is also determined by a variety of additional factors including solvent effects and energetics of solvation, chelate ring size, and “hard/soft” complementarity. The emission responses of **2** and **4** to Hg<sup>2+</sup> and Cu<sup>2+</sup>, respectively, have also been compared (Supporting Information). Incremental quenching (due to spin–orbit interactions and paramagnetic nature, respectively)<sup>36</sup> is observed in both cases, but while the peak maximum for **4** remains constant, blue-shifted emissions are apparent for **2** upon addition of Hg<sup>2+</sup> and Cu<sup>2+</sup> (from  $\lambda_{\text{max}}$  630 to 617 and 620 nm, respectively, for up to 2 equiv; compared with  $\lambda_{\text{max}}$  605 nm with enhancement for Pb<sup>2+</sup>). The less blue-shifted emissions for **2** are tentatively ascribed to limited Hg<sup>2+</sup>/Cu<sup>2+</sup>...O(salphen) interactions leading to destabilization of the O(p)→ $\pi^*$ (diimine) transition, but the Hg<sup>2+</sup> and Cu<sup>2+</sup> ions (radius = 1.02 and 0.73 Å, respectively)<sup>37</sup> evidently do not match the characteristics and dimensions of the O<sub>4</sub>-cavity (as indicated by ESI–MS), and hence the weak intramolecular  $\pi$ -interactions and associated self-quenching can persist. In contrast, the <sup>t</sup>Bu substituents in **4** would impede coordination by the O(salphen) groups, and the quenched emission is therefore not blue-shifted. Overall, the evidence in this work suggests that a shape-persistent (Pt-salphen)<sub>2</sub> framework bearing a suitable binding cavity can afford a blue-shifted and enhanced emission response for selected ions (Pb<sup>2+</sup>).

## CONCLUSION

The M<sup>2+</sup>-binding properties of shape-persistent (M-salphen)<sub>2</sub> (M = Pt, Zn) complexes, which may be considered as phosphorescent relatives of calix[4]arene, have been investigated. Differences in fluid photophysical properties are attributed to the combined effects of the metal centers, substituents on the salphen moieties, and to some extent intramolecular  $\pi$ -stacking interactions. The cation-induced photophysical responses of the Pt<sub>2</sub> coordination frameworks may be ascribed to host–guest interactions, the nature of which is determined by the propensity of the xanthene-appended Pt-salphen units to undergo axial rotation to create an O<sub>4</sub>-cavity that is capable of (and indeed complementary for) binding selected guests, in this case Pb<sup>2+</sup>. Evidence in support of the binding mechanism has been gathered from ESI–MS experiments, DFT calculations, and quantitative spectrophotometric titrations, plus comparative studies with control complexes. The present binuclear system is structurally versatile, and astute modifications may lead to novel properties and applications.

## EXPERIMENTAL SECTION

**General Considerations.** Solvents for syntheses (analytical grade) were used without further purification, and all metalation reactions were performed under a nitrogen atmosphere. Solvents for photophysical measurements were purified according to conventional methods. <sup>1</sup>H NMR spectra were obtained on Bruker DRX 300 and 400 FT-NMR spectrometers (ppm) using Me<sub>4</sub>Si as internal standard. ESI mass spectra were measured on a Perkin-Elmer SCIEX API 365 mass spectrometer. Elemental analyses were performed on a Vario EL elemental analyzer (Elementar Analysensysteme GmbH). Synthetic procedures for the ligand precursors and mononuclear complexes are given in the Supporting Information.

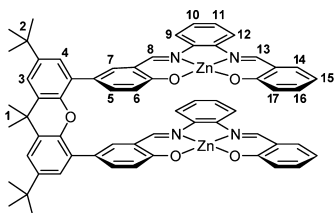
UV–vis absorption spectra were obtained on an Agilent 8453 diode array spectrophotometer. Steady-state emission spectra were recorded on a SPEX FluoroLog 3-TCSPC spectrophotometer equipped with a Hamamatsu R928 PMT detector, and emission lifetime measurements were conducted using NanoLed sources in the fast MCS mode and checked using the TCSPC mode. Sample and standard solutions were degassed with at least three freeze–pump–thaw cycles. Low-temperature (77 K) emission spectra for glasses and solid-state samples were recorded in 5 mm diameter quartz tubes, which were placed in a liquid nitrogen Dewar equipped with quartz windows. The emission quantum yield was measured by using [Ru(bpy)<sub>3</sub>](PF<sub>6</sub>)<sub>2</sub> in degassed acetonitrile as the standard ( $\Phi_r = 0.062$ ) and calculated by:  $\Phi_s = \Phi_r(B_s/B_r)(n_r/n_s)^2(D_s/D_r)$ , where the subscripts s and r refer to sample and reference standard solution, respectively,  $n$  is the refractive index of the solvents,  $D$  is the integrated intensity, and  $\Phi$  is the luminescence quantum yield. The quantity  $B$  is calculated by the equation  $B = 1 - 10^{-AL}$ , where  $A$  is the absorbance at the excitation wavelength and  $L$  is the optical path length. Errors for  $\lambda$  ( $\pm 1$  nm),  $\tau$  ( $\pm 10\%$ ), and  $\Phi$  ( $\pm 10\%$ ) are estimated. Solutions of Pt(II) (CHCl<sub>3</sub>/CH<sub>3</sub>CN, 1/1) and Zn(II) (CH<sub>3</sub>CN) complexes, and metal perchlorate salts (CH<sub>3</sub>CN), were prepared in solvents of spectroscopic grade. Absorption and emission titrations were carried out in a quartz cuvette by addition of small volumes of metal ion solutions ( $5 \times 10^{-3}$  M) to the Pt(II) or Zn(II) complex.

Crystals data were collected on an Oxford Diffraction Gemini S Ultra X-ray single-crystal diffractometer using graphite-monochromated Cu K $\alpha$  radiation ( $\lambda = 1.5418$  Å). The structures were solved by direct methods and refined using the SHELXL-97 program on a PC.<sup>38</sup> For **4**, electron density attributable to additional solvent molecules in the unit cell was removed using the PLATON (SQUEEZE) program.<sup>39</sup> DFT calculations on molecular structures were performed at the B3LYP level with the CEP-31G basis set using the Gaussian 09 program package.<sup>40</sup> In each case, the energy-minimized calculated structure was confirmed to be a minimum from vibrational frequency calculations.

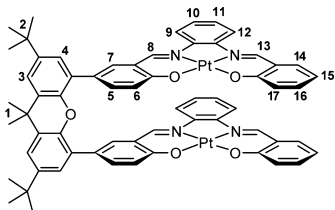
**Synthesis. Complex 1.** Compound **L2** (0.200 g, 0.355 mmol in powder form) and triethylamine (1 mL) were added to a stirred solution



of **L3** (0.151 g, 0.711 mmol) and zinc acetate dihydrate (0.172 g, 0.782 mmol) in MeOH (10 mL) at room temperature. The reaction mixture became an orange suspension after stirring at room temperature for 30 min under air, and a yellow suspension was formed after 20 h. The crude product was filtered and copiously washed with MeOH, and recrystallization by slow evaporation of THF afforded **1** (0.230 g, 60%) as a bright yellow solid. Anal. Calcd for  $C_{63}H_{54}N_4O_5Zn_2 \cdot (H_2O)_6$  (1186.04): C, 63.80; H, 5.61; N, 4.72. Found: C, 63.68; H, 5.22; N, 4.51.  $^1H$  NMR (400 MHz,  $d_6$ -DMSO):  $\delta$  8.84 (s, 2H,  $H^{13}$ ),  $\delta$  8.77 (s, 2H,  $H^8$ ), 7.77–7.73 (m, 4H,  $H^9$ ,  $H^{12}$ ), 7.50 (d,  $J$  = 2.2 Hz, 2H,  $H^7$ ), 7.43 (d,  $J$  = 2.2 Hz, 2H,  $H^3$ ), 7.42 (dd,  $J$  = 8.9, 2.3 Hz, 2H,  $H^5$ ), 7.31 (dd,  $J$  = 7.9, 1.4 Hz, 2H,  $H^{14}$ ), 7.25–7.18 (m, 6H,  $H^4$ ,  $H^{10}$ ,  $H^{11}$ ), 7.16–7.12 (m, 2H,  $H^{16}$ ), 6.54 (d,  $J$  = 8.5 Hz, 2H,  $H^{17}$ ), 6.52–6.49 (m, 2H,  $H^{15}$ ), 6.45 (d,  $J$  = 8.8 Hz, 2H,  $H^6$ ), 1.71 (s, 6H,  $H^1$ ), 1.36 (s, 18H,  $H^2$ ). ESI–MS (+ve mode):  $m/z$  1079  $[M + H]^+$ .

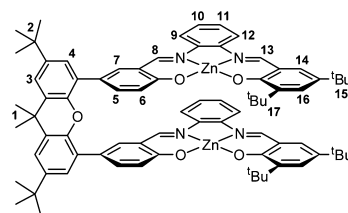


**Complex 2.** A solution of  $PtCl_2$  (67.4 mg, 0.253 mmol) in DMSO (5 mL) was added to a yellow solution of **1** (0.130 g, 0.121 mmol) in THF/DMSO (1:2, 15 mL). The reaction mixture was stirred at 90 °C for 7 d to give a dark red suspension. After cooling to room temperature, the suspension was diluted with  $CH_2Cl_2$  (100 mL), washed with water (4  $\times$  100 mL), and dried over  $MgSO_4$ . The resultant solution was filtered and concentrated to dryness. The crude product was purified by column chromatography ( $Al_2O_3$ , gradient elution from 50%  $CH_2Cl_2$  in hexane to THF), then washed with diethyl ether, and finally precipitated from hot  $CHCl_3$  to give **2** (83.0 mg, 51%) as a red solid. Anal. Calcd for  $C_{63}H_{54}N_4O_5Pt_2 \cdot (H_2O)_4$  (1409.34): C, 53.69; H, 4.43; N, 3.98. Found: C, 53.32; H, 4.01; N, 3.72.  $^1H$  NMR (400 MHz,  $d_6$ -DMSO):  $\delta$  8.70 (s, 2H,  $H^{13}$ ), 8.22–8.20 (m, 4H,  $H^8$ ,  $H^{12}$ ), 7.91–7.89 (m, 2H,  $H^9$ ), 7.76 (d,  $J$  = 2.3 Hz, 2H,  $H^7$ ), 7.72 (dd,  $J$  = 8.8, 2.4 Hz, 2H,  $H^5$ ), 7.50 (d,  $J$  = 2.3 Hz, 2H,  $H^3$ ), 7.40–7.34 (m, 6H,  $H^{10}$ ,  $H^{11}$ ,  $H^{16}$ ), 7.28 (d,  $J$  = 2.3 Hz, 2H,  $H^{14}$ ), 7.07–7.05 (m, 2H,  $H^{17}$ ), 6.75 (d,  $J$  = 8.4 Hz, 2H,  $H^{15}$ ), 6.66 (d,  $J$  = 8.8 Hz, 2H,  $H^6$ ), 6.41 (m, 2H,  $H^{15}$ ), 1.77 (s, 6H,  $H^1$ ), 1.37 (s, 18H,  $H^2$ ). ESI–MS (+ve mode):  $m/z$  1359  $[M + Na]^+$ .

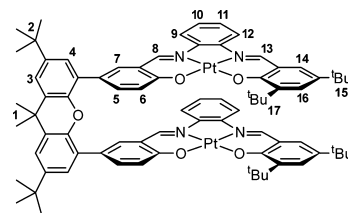


**Complex 3.** Compound **L2** (30 mg, 0.053 mmol in powder form) and triethylamine (2 mL) were added to a stirred solution of **L4** (35 mg, 0.11 mmol) and zinc acetate dihydrate (27 mg, 0.12 mmol) in MeOH (20 mL) at room temperature. The reaction mixture became an orange suspension after stirring at room temperature for 30 min under air, and was allowed to stir at reflux for 20 h. The crude product was filtered and copiously washed with cooled MeOH. Precipitation from  $CH_2Cl_2$ /hexane (1:9) afforded **3** (50 mg, 72%) as a bright yellow solid. Anal. Calcd for  $C_{79}H_{86}N_4O_5Zn_2 \cdot (CH_2Cl_2)_5$  (1727.03): C, 58.42; H, 5.60; N, 3.24. Found: C, 58.86; H, 5.89; N, 2.85.  $^1H$  NMR (400 MHz,  $CD_2Cl_2$ ):  $\delta$  8.73 (s, 2H,  $H^{13}$ ), 8.45 (s, 2H,  $H^8$ ), 7.68 (d,  $J$  = 7.3 Hz, 2H,  $H^{12}$ ), 7.62 (d,  $J$  = 7.2 Hz, 2H,  $H^9$ ), 7.47–7.45 (m, 2H,  $H^{11}$ ), 7.43 (d,  $J$  = 2.1 Hz, 2H,  $H^3$ ), 7.41–7.38 (m, 2H,  $H^{10}$ ), 7.37 (d,  $J$  = 2.7 Hz, 2H,  $H^{16}$ ), 7.22 (d,  $J$  = 2.2 Hz, 2H,  $H^4$ ), 7.19 (dd,  $J$  = 8.5, 2.4 Hz, 2H,  $H^5$ ), 7.09 (d,  $J$  = 2.8 Hz, 2H,  $H^{14}$ ), 7.08 (d,  $J$  = 2.4 Hz, 2H,  $H^7$ ), 6.48 (d,  $J$  = 8.5 Hz, 2H,  $H^6$ ), 1.77 (s, 6H,  $H^1$ ), 1.37 (s, 18H,  $H^2$ ), 1.34 (s, 18H,  $H^{17}$ ), 1.30 (s, 18H,  $H^{15}$ ).  $^{13}C$  NMR (101 MHz,  $CD_2Cl_2$ ): 170.5, 168.1, 164.2, 162.9, 146.1, 145.6, 141.1, 141.1, 139.8, 139.3, 135.5, 134.6, 130.5, 130.3, 123.0, 128.3, 127.3,

125.5, 124.8, 121.5, 121.3, 119.3, 118.9, 116.7, 116.2, 35.8, 35.5, 34.9, 34.1, 32.0, 31.8, 31.5, 29.6. ESI–MS (+ve mode):  $m/z$  1304  $[M + H]^+$ .



**Complex 4.** A solution of  $PtCl_2$  (0.17 g, 0.64 mmol) in DMSO (20 mL) was added to a solution of **3** (0.38 g, 0.29 mmol) in DMSO (30 mL). The reaction mixture was stirred at 90 °C for 14 d. The resultant mixture was diluted with  $CH_2Cl_2$  and washed with  $H_2O$ . The organic layer was separated, dried over  $MgSO_4$ , and filtered. The filtrate was concentrated in vacuo, and the residual was purified by column chromatography ( $SiO_2$ , 50%  $CH_2Cl_2$  in hexane) and washed with MeOH to give **4** (0.40 g, 88%) as a red solid. Anal. Calcd for  $C_{79}H_{86}N_4O_5Pt_2 \cdot (H_2O)$  (1579.72): C, 60.06; H, 5.61; N, 3.55. Found: C, 60.02; H, 5.43; N, 3.31.  $^1H$  NMR (400 MHz,  $CD_2Cl_2$ ):  $\delta$  8.32 (s, 2H,  $H^{13}$ ), 7.83–7.78 (m, 4H,  $H^8$ ,  $H^7$ ), 7.71 (s, 2H,  $H^9$ ), 7.60 (d,  $J$  = 7.8 Hz, 2H,  $H^{12}$ ), 7.55 (d,  $J$  = 2.3 Hz, 2H,  $H^{16}$ ), 7.52 (d,  $J$  = 8.1 Hz, 2H,  $H^9$ ), 7.46 (d,  $J$  = 2.2 Hz, 2H,  $H^3$ ), 7.34 (d,  $J$  = 2.2 Hz, 2H,  $H^4$ ), 7.27–7.18 (m, 4H,  $H^{10}$ ,  $H^{11}$ ), 6.93 (d,  $J$  = 8.8 Hz, 2H,  $H^6$ ), 6.91 (d,  $J$  = 2.3 Hz, 2H,  $H^{14}$ ), 1.79 (s, 6H,  $H^1$ ), 1.41 (s, 18H,  $H^2$ ), 1.36 (s, 18H,  $H^{17}$ ), 1.29 (s, 18H,  $H^{15}$ ).  $^{13}C$  NMR (101 MHz,  $CD_2Cl_2$ ): 164.8, 164.0, 149.0, 148.2, 146.0, 145.9, 145.3, 145.2, 141.1, 137.3, 137.1, 136.2, 130.9, 129.9, 127.9, 127.8, 127.8, 126.6, 125.9, 125.3, 122.7, 122.1, 121.8, 121.2, 115.9, 115.7, 36.1, 35.2, 34.9, 34.2, 33.5, 31.7, 31.4, 30.3. ESI–MS (+ve mode):  $m/z$  1585  $[M + Na]^+$ .



## ■ ASSOCIATED CONTENT

### Supporting Information

Listings of experimental details and characterization data; crystal data and refinement details for **4**, **7**, and **8**; molecular structure of **8**; additional photophysical data, spectra, and responses and curve fittings for substrate binding; and details of DFT calculations. This material is available free of charge via the Internet at <http://pubs.acs.org>.

## ■ AUTHOR INFORMATION

### Corresponding Author

\*E-mail: [mcwchan@cityu.edu.hk](mailto:mcwchan@cityu.edu.hk).

### Notes

The authors declare no competing financial interest.

## ■ ACKNOWLEDGMENTS

This work was fully supported by a grant from the Research Grants Council of the Hong Kong SAR, China (CityU 100212). We are grateful to the reviewers for helpful comments.

## ■ REFERENCES

- (a) Mizuno, T.; Wei, W.-H.; Eller, L. R.; Sessler, J. L. *J. Am. Chem. Soc.* **2002**, *124*, 1134. (b) Goshe, A. J.; Steele, I. M.; Bosnich, B. *J. Am. Chem. Soc.* **2003**, *125*, 444. (c) Klärner, F.-G.; Kahlert, B. *Acc. Chem. Res.*

- 2003, 36, 919. (d) Chebny, V. J.; Rathore, R. J. *Am. Chem. Soc.* **2007**, 129, 8458. (e) Ulrich, S.; Lehn, J.-M. *Chem.-Eur. J.* **2009**, 15, 5640. (f) Hong, Y.; Lam, J. W. Y.; Tang, B. Z. *Chem. Commun.* **2009**, 4332. (g) Dutta, S.; Bučar, D.-K.; MacGillivray, L. R. *Org. Lett.* **2011**, 13, 2260. (h) Iwaniuk, D. P.; Wolf, C. J. *Am. Chem. Soc.* **2011**, 133, 2414. (i) Pochorowski, I.; Ebert, M.-O.; Gisselbrecht, J.-P.; Boudon, C.; Schweizer, W. B.; Diederich, F. J. *Am. Chem. Soc.* **2012**, 134, 14702.
- (2) (a) Nakano, T.; Yade, T. J. *Am. Chem. Soc.* **2003**, 125, 15474. (b) Nguyen, T.-Q.; Martel, R.; Avouris, P.; Bushey, M. L.; Brus, L.; Nuckolls, C. J. *Am. Chem. Soc.* **2004**, 126, 5234. (c) Yoo, H.; Yang, J.; Yousef, A.; Wasielewski, M. R.; Kim, D. J. *Am. Chem. Soc.* **2010**, 132, 3939. (d) He, J.; Crase, J. L.; Wadumethrige, S. H.; Thakur, K.; Dai, L.; Zou, S.; Rathore, R.; Hartley, C. S. J. *Am. Chem. Soc.* **2010**, 132, 13848. (e) Ohta, E.; Sato, H.; Ando, S.; Kosaka, A.; Fukushima, T.; Hashizume, D.; Yamasaki, M.; Hasegawa, K.; Muraoka, A.; Ushiyama, H.; Yamashita, K.; Aida, T. *Nat. Chem.* **2011**, 3, 68. (f) Schlütter, F.; Rossel, F.; Kivala, M.; Enkelmann, V.; Gisselbrecht, J.-P.; Ruffieux, P.; Fasel, R.; Müllen, K. J. *Am. Chem. Soc.* **2013**, 135, 4550.
- (3) (a) Liu, S.-Y.; Nocera, D. G. J. *Am. Chem. Soc.* **2005**, 127, 5278. (b) Lee, C. H.; Dogutan, D. K.; Nocera, D. G. J. *Am. Chem. Soc.* **2011**, 133, 8775. (c) Dogutan, D. K.; McGuire, R., Jr.; Nocera, D. G. J. *Am. Chem. Soc.* **2011**, 133, 9178. (d) Gianneschi, N. C.; Cho, S.-H.; Nguyen, S. T.; Mirkin, C. A. *Angew. Chem., Int. Ed.* **2004**, 43, 5503.
- (4) (a) McFarland, S. A.; Finney, N. S. J. *Am. Chem. Soc.* **2001**, 123, 1260. (b) McFarland, S. A.; Finney, N. S. J. *Am. Chem. Soc.* **2002**, 124, 1178. (c) Barboiu, M.; Prodi, L.; Montalti, M.; Zaccaroni, N.; Kyrtsakas, N.; Lehn, J.-M. *Chem.-Eur. J.* **2004**, 10, 2953. (d) Mei, X.; Wolf, C. J. *Am. Chem. Soc.* **2004**, 126, 14736. (e) Mello, J. V.; Finney, N. S. J. *Am. Chem. Soc.* **2005**, 127, 10124. (f) Wolf, C.; Liu, S.; Reinhardt, B. C. *Chem. Commun.* **2006**, 4242.
- (5) (a) Kleij, A. W. *Chem.-Eur. J.* **2008**, 14, 10520. (b) Whiteoak, C. J.; Salassa, G.; Kleij, A. W. *Chem. Soc. Rev.* **2012**, 41, 622.
- (6) (a) Ma, C. T. L.; MacLachlan, M. J. *Angew. Chem., Int. Ed.* **2005**, 44, 4178. (b) Houjou, H.; Ito, M.; Araki, K. *Inorg. Chem.* **2009**, 48, 10703. (c) Chong, J. H.; Jooya Ardakani, S.; Smith, K. J.; MacLachlan, M. J. *Chem.-Eur. J.* **2009**, 15, 11824. (d) Consiglio, G.; Failla, S.; Finocchiaro, P.; Oliveri, I. P.; Purrello, R.; Di Bella, S. *Inorg. Chem.* **2010**, 49, 5134. (e) Dömer, J.; Slootweg, J. C.; Hupka, F.; Lammertsma, K.; Hahn, F. E. *Angew. Chem., Int. Ed.* **2010**, 49, 6430. (f) Frischmann, P. D.; Facey, G. A.; Ghi, P. Y.; Gallant, A. J.; Bryce, D. L.; Lelj, F.; MacLachlan, M. J. *J. Am. Chem. Soc.* **2010**, 132, 3893. (g) Escárcega-Bobadilla, M. V.; Salassa, G.; Martínez Belmonte, M.; Escudero-Adán, E. C.; Kleij, A. W. *Chem.-Eur. J.* **2012**, 18, 6805.
- (7) (a) Cametti, M.; Nissinen, M.; Dalla Cort, A.; Mandolini, L.; Rissanen, K. J. *Am. Chem. Soc.* **2005**, 127, 3831. (b) Akine, S.; Taniguchi, T.; Nabeshima, T. J. *Am. Chem. Soc.* **2006**, 128, 15765. (c) Libra, E. R.; Scott, M. J. *Chem. Commun.* **2006**, 1485. (d) Germain, M. E.; Vargo, T. R.; Khalifah, P. G.; Knapp, M. J. *Inorg. Chem.* **2007**, 46, 4422. (e) Chen, C.-T.; Lin, Y.-H.; Kuo, T.-S. J. *Am. Chem. Soc.* **2008**, 130, 12842.
- (8) (a) Li, G.; Yu, W.; Ni, J.; Liu, T.; Liu, Y.; Sheng, E.; Cui, Y. *Angew. Chem., Int. Ed.* **2008**, 47, 1245. (b) Wezenberg, S. J.; Salassa, G.; Escudero-Adán, E. C.; Benet-Buchholz, J.; Kleij, A. W. *Angew. Chem., Int. Ed.* **2011**, 50, 713.
- (9) (a) Leung, A. C. W.; Hui, J. K.-H.; Chong, J. H.; MacLachlan, M. J. *Dalton Trans.* **2009**, 5199. (b) Komiya, N.; Muraoka, T.; Iida, M.; Miyayama, M.; Takahashi, K.; Naota, T. J. *Am. Chem. Soc.* **2011**, 133, 16054. (c) Dunn, T. J.; Ramogida, C. F.; Simmonds, C.; Paterson, A.; Wong, E. W. Y.; Chiang, L.; Shimazaki, Y.; Storr, T. *Inorg. Chem.* **2011**, 50, 6746.
- (10) (a) Leung, A. C. W.; MacLachlan, M. J. *J. Mater. Chem.* **2007**, 17, 1923. (b) Hui, J. K.-H.; Yu, Z.; Mirfakhrai, T.; MacLachlan, M. J. *Chem.-Eur. J.* **2009**, 15, 13456. (c) Hui, J. K.-H.; Frischmann, P. D.; Tso, C.-H.; Michal, C. A.; MacLachlan, M. J. *Chem.-Eur. J.* **2010**, 16, 2453. (d) Frischmann, P. D.; Guieu, S.; Tabeshi, R.; MacLachlan, M. J. *J. Am. Chem. Soc.* **2010**, 132, 7668.
- (11) (a) Martínez Belmonte, M.; Wezenberg, S. J.; Haak, R. M.; Anselmo, D.; Escudero-Adán, E. C.; Benet-Buchholz, J.; Kleij, A. W. *Dalton Trans.* **2010**, 39, 4541. (b) Salassa, G.; Coenen, M. J. J.; Wezenberg, S. J.; Hendriksen, B. L. M.; Speller, S.; Elemans, J. A. A. W.; Kleij, A. W. J. *Am. Chem. Soc.* **2012**, 134, 7186.
- (12) (a) Guo, Z.; Chan, M. C. W. *Chem.-Eur. J.* **2009**, 15, 12585. (b) Tong, W.-L.; Lai, L.-M.; Chan, M. C. W. *Dalton Trans.* **2008**, 1412. (13) Sun, S.; Tong, W.-L.; Chan, M. C. W. *Macromol. Rapid Commun.* **2010**, 31, 1965.
- (14) Tong, W.-L.; Chan, M. C. W.; Yiu, S.-M. *Organometallics* **2010**, 29, 6377.
- (15) (a) Guo, Z.; Tong, W.-L.; Chan, M. C. W. *Chem. Commun.* **2009**, 6189. (b) Guo, Z.; Yiu, S.-M.; Chan, M. C. W. *Chem.-Eur. J.* **2013**, DOI: 10.1002/chem.201300421.
- (16) (a) Lai, S.-W.; Chan, M. C. W.; Cheung, T.-C.; Peng, S.-M.; Che, C.-M. *Inorg. Chem.* **1999**, 38, 4046. (b) Wong, K. H.; Chan, M. C. W.; Che, C.-M. *Chem.-Eur. J.* **1999**, 5, 2845. (c) Wu, P.; Ma, D.-L.; Leung, C.-H.; Yan, S.-C.; Zhu, N.; Abagyan, R.; Che, C.-M. *Chem.-Eur. J.* **2009**, 15, 13008.
- (17) (a) Lin, Y.-Y.; Chan, S.-C.; Chan, M. C. W.; Hou, Y.-J.; Zhu, N.; Che, C.-M.; Liu, Y.; Wang, Y. *Chem.-Eur. J.* **2003**, 9, 1263. (b) Che, C.-M.; Chan, S.-C.; Xiang, H.-F.; Chan, M. C. W.; Liu, Y.; Wang, Y. *Chem. Commun.* **2004**, 1484. (c) Che, C.-M.; Kwok, C.-C.; Lai, S.-W.; Rausch, A. F.; Finkenzeller, W. J.; Zhu, N.; Yersin, H. *Chem.-Eur. J.* **2010**, 16, 233.
- (18) (a) Kleij, A. W.; Tooke, D. M.; Spek, A. L.; Reek, J. N. H. *Eur. J. Inorg. Chem.* **2005**, 4626. (b) Castilla, A. M.; Curreli, S.; Escudero-Adán, E. C.; Belmonte, M.; Benet-Buchholz, J.; Kleij, A. W. *Org. Lett.* **2009**, 11, 5218.
- (19) Escudero-Adán, E. C.; Benet-Buchholz, J.; Kleij, A. W. *Inorg. Chem.* **2007**, 46, 7265.
- (20) San Felices, L.; Escudero-Adán, E. C.; Benet-Buchholz, J.; Kleij, A. W. *Inorg. Chem.* **2009**, 48, 846.
- (21) Chang, K.-H.; Huang, C.-C.; Liu, Y.-H.; Hu, Y.-H.; Chou, P.-T.; Lin, Y.-C. *Dalton Trans.* **2004**, 1731.
- (22) (a) Miskowski, V. M.; Houlding, V. H. *Inorg. Chem.* **1991**, 30, 4446. (b) Novoa, J. J.; Aullón, G.; Alemany, P.; Alvarez, S. J. *Am. Chem. Soc.* **1995**, 117, 7169. (c) Lu, W.; Chan, M. C. W.; Zhu, N.; Che, C.-M.; Li, C.; Hui, Z. J. *Am. Chem. Soc.* **2004**, 126, 7639.
- (23) (a) Lu, W.; Chan, M. C. W.; Cheung, K.-K.; Che, C.-M. *Organometallics* **2001**, 20, 2477. (b) Lai, S.-W.; Lam, H.-W.; Lu, W.; Cheung, K.-K.; Che, C.-M. *Organometallics* **2002**, 21, 226.
- (24) (a) Singer, A. L.; Atwood, D. A. *Inorg. Chim. Acta* **1998**, 277, 157. (b) Reglinski, J.; Morris, S.; Stevenson, D. *Polyhedron* **2002**, 21, 2175. (c) Kleij, A. W.; Kuil, M.; Lutz, M.; Tooke, D. M.; Spek, A. L.; Kamer, P. C. J.; van Leeuwen, P. W. N. M.; Reek, J. N. H. *Inorg. Chim. Acta* **2006**, 359, 1807.
- (25) The parameter  $\tau$ , defined as  $(\beta - \alpha)/60$ , is applicable to 5-coordinate structures to reflect the structural continuum between trigonal bipyramidal and tetragonal pyramidal;  $\tau$  is zero for a perfect tetragonal geometry and becomes unity for a perfect trigonal bipyramidal geometry: Addison, A. W.; Rao, T. N.; Reedijk, J.; van Rijn, J.; Verschoor, G. C. J. *Chem. Soc., Dalton Trans.* **1984**, 1349. For complex **7**, the largest angles amongst the four atoms O1, O2, N1, N2 are  $\beta = 165.75(5)^\circ$  for O1–Zn1–N2, and  $\alpha = 147.27(5)^\circ$  for O2–Zn1–N1; thus  $\tau$  is  $(165.75 - 147.27)/60 = 0.308$ .
- (26) (a) Ballardini, R.; Varani, G.; Indelli, M. T.; Scandola, F. *Inorg. Chem.* **1986**, 25, 3858. (b) Cummings, S. D.; Eisenberg, R. J. *Am. Chem. Soc.* **1996**, 118, 1949. (c) Donges, D.; Nagle, J. K.; Yersin, H. *Inorg. Chem.* **1997**, 36, 3040.
- (27) (a) Splan, K. E.; Massari, A. M.; Morris, G. A.; Sun, S.-S.; Reina, E.; Nguyen, S. T.; Hupp, J. T. *Eur. J. Inorg. Chem.* **2003**, 2348. (b) Kuo, K.-L.; Huang, C.-C.; Lin, Y.-C. *Dalton Trans.* **2008**, 3889.
- (28) (a) Hernández-Molina, R.; Mederos, A.; Gill, P.; Domínguez, S.; Núñez, P.; Germain, G.; Debaerdemaeker, T. *Inorg. Chim. Acta* **1997**, 256, 319. (b) Sánchez, M.; Harvey, M. J.; Nordstrom, F.; Parkin, S.; Atwood, D. A. *Inorg. Chem.* **2002**, 41, 5397. (c) Darensbourg, D. J.; Choi, W.; Karroonnirun, O.; Bhuvanesh, N. *Macromolecules* **2008**, 41, 3493.
- (29) Results from ESI-MS studies of **1** with  $Mg^{2+}$  ions (3 equiv) in  $CH_3CN$  indicated possible transmetalation and demetalation processes.
- (30) Bourson, J.; Pouget, J.; Valeur, B. J. *Phys. Chem.* **1993**, 97, 4552.

- (31) Cooperative 2:2 binding, which would afford 0.25 amu separations, can therefore be discounted (nonsigmoidal binding curve also gives excellent fit for 1:1 binding).
- (32) Carbonaro, L.; Isola, M.; La Pegna, P.; Senatore, L.; Marchetti, F. *Inorg. Chem.* **1999**, *38*, 5519.
- (33) Berenguer, J. R.; Díez, A.; Fernández, J.; Forniés, J.; García, A.; Gil, B.; Lalinde, E.; Moreno, M. T. *Inorg. Chem.* **2008**, *47*, 7703.
- (34) Marandi, F.; Rutvand, R.; Rafiee, M.; Goh, J. H.; Fun, H.-K. *Inorg. Chim. Acta* **2010**, *363*, 4000.
- (35) Coordination of Pb(II) by Lewis-basic Pt(0) has been reported: Heitmann, D.; Pape, T.; Hepp, A.; Mück-Lichtenfeld, C.; Grimme, S.; Hahn, F. E. *J. Am. Chem. Soc.* **2011**, *133*, 11118.
- (36) (a) McClure, D. S. *J. Chem. Phys.* **1949**, *17*, 905. (b) Hercules, D. M. In *Fluorescence and Phosphorescence Analysis*; Hercules, D. M., Ed.; John Wiley & Sons: New York, 1966; Chapter 1. (c) Balch, A. L.; Catalano, V. J.; Chatfield, M. A.; Nagle, J. K.; Olmstead, M. M.; Reedy, P. E., Jr. *J. Am. Chem. Soc.* **1991**, *113*, 1252. (d) Koike, T.; Watanabe, T.; Aoki, S.; Kimura, E.; Shiro, M. *J. Am. Chem. Soc.* **1996**, *118*, 12696. (e) Lee, H.; Lee, H.-S.; Reibenspies, J. H.; Hancock, R. D. *Inorg. Chem.* **2012**, *51*, 10904.
- (37) Shannon, R. D. *Acta Crystallogr.* **1976**, *A32*, 751.
- (38) Sheldrick, G. M. *SHELXS-97 and SHELXL-97, Programs for Crystal Structure Solution and Refinement*; University of Göttingen: Göttingen, Germany, 1997.
- (39) Spek, A. L. *J. Appl. Crystallogr.* **2003**, *36*, 7.
- (40) Frisch, M. J.; et al. *Gaussian 09*, revision B.1; Gaussian, Inc.: Wallingford, CT, 2009.